ACS Synthetic Biology

Research Article

pubs.acs.org/synthbio

CRISPR Perturbation of Gene Expression Alters Bacterial Fitness under Stress and Reveals Underlying Epistatic Constraints

Peter B. Otoupal,[†] Keesha E. Erickson,[†] Antoni Escalas-Bordoy,[†] and Anushree Chatterjee*[,†,‡]

[†]Department of Chemical and Biological Engineering, University of Colorado at Boulder, Boulder, Colorado 80309, United States
[‡]BioFrontiers Institute, University of Colorado at Boulder, Boulder, Colorado 80309, United States

Supporting Information

ABSTRACT: The evolution of antibiotic resistance has engendered an impending global health crisis that necessitates a greater understanding of how resistance emerges. The impact of nongenetic factors and how they influence the evolution of resistance is a largely unexplored area of research. Here we present a novel application of CRISPR-Cas9 technology for investigating how gene expression governs the adaptive pathways available to bacteria during the evolution of resistance. We examine the impact of gene expression changes on bacterial adaptation by constructing a library of deactivated CRISPR-Cas9 synthetic devices to tune the expression of a set of stress-response genes in *Escherichia coli*. We show that artificially inducing perturbations in gene expression imparts significant synthetic control over fitness and growth during stress exposure. We present evidence that these impacts are reversible; strains with synthetically perturbed gene expression regained wild-type growth phenotypes upon stress removal, while maintaining divergent growth characteristics under stress. Furthermore, we demonstrate a prevailing trend toward negative epistatic interactions when multiple gene perturbations are combined simultaneously, thereby posing an intrinsic constraint on gene expression underlying adaptive trajectories. Together, these results emphasize how CRISPR-Cas9 can be employed to engineer gene expression changes that shape bacterial adaptation, and present a novel approach to synthetically control the evolution of antimicrobial resistance.

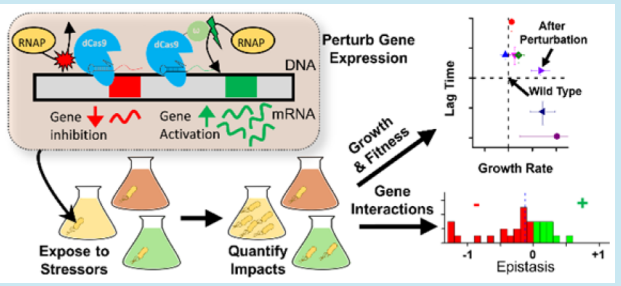

KEYWORDS: *CRISPR, transcriptome, adaptive evolution, epistasis, antibiotic resistance*

As bacteria continue to demonstrate their ability to adapt to a broad range of antibiotics[1] and other antimicrobials,[2] a dearth of effective treatments for life-threatening pathogenic infections has become a prominent concern.[3] Although genomic divergences (*i.e.*, mutations) have been the focus of conventional adaptive evolutionary research, the impact of variations in gene expression on microbial evolution during stress exposure[4−6] is a relatively unexplored field. Heterogeneous gene expression has been shown to enable bacterial bet-hedging[7] strategies to create diversity in order to dynamically respond to sudden environmental stressors.[6] This mutation-independent process, known as adaptive resistance,[8] could expedite the evolution of antimicrobial resistance. Supporting this notion is the observance of distinct changes in bacterial transcriptomes during exposure to antibiotics[9] and disinfectants,[10] as well as significant heterogeneity in interpopulation gene expression during the first hundred or so generations of adapting bacterial populations.[11−13]

In this study, we take inspiration from these adaptive strategies found in nature, and hypothesize that synthetically inducing small perturbations in gene expression can enable artificial control over both positive and negative fitness phenotypes in adapting strains. Assuming that gene expression is normally distributed around basal levels in a bacterial population, we hypothesize small changes in the distribution of gene expression could exacerbate the pre-existing growth and fitness phenotypes of subpopulations with altered gene expression (Figure 1A). Further, we hypothesize that the simultaneous perturbation of multiple genes can induce unique phenotypic responses via epistatic interactions. Negative epistatic interactions, where the combined fitness benefits of simultaneous mutations are less than expected, have been shown to either overshadow positive epistasis during adaptation[14,15] to environmental conditions or impact long-term evolvability.[16] While it has been suggested that the epigenetic epistatic interactions of gene expression ultimately constrain long-term evolution,[17] very little is understood regarding how these interactions might impact the early stages of adaptive resistance.

To investigate our hypotheses, we engineered deactivated CRISPR (Clustered Regularly Interspaced Short Palindromic Repeats)-associated protein 9 (dCas9) based genomic devices to synthetically induce small perturbations in the transcriptome of *Escherichia coli* (*E. coli*). This presents a novel application of CRISPR technology as we employ it to explore the impact of subtle gene expression changes on bacterial fitness in the presence of sub-lethal levels of stressors, and to the best of our

Received: February 5, 2016

DOI: 10.1021/acssynbio.6b00050
ACS Synth. Biol. XXXX, XXX, XXX−XXX

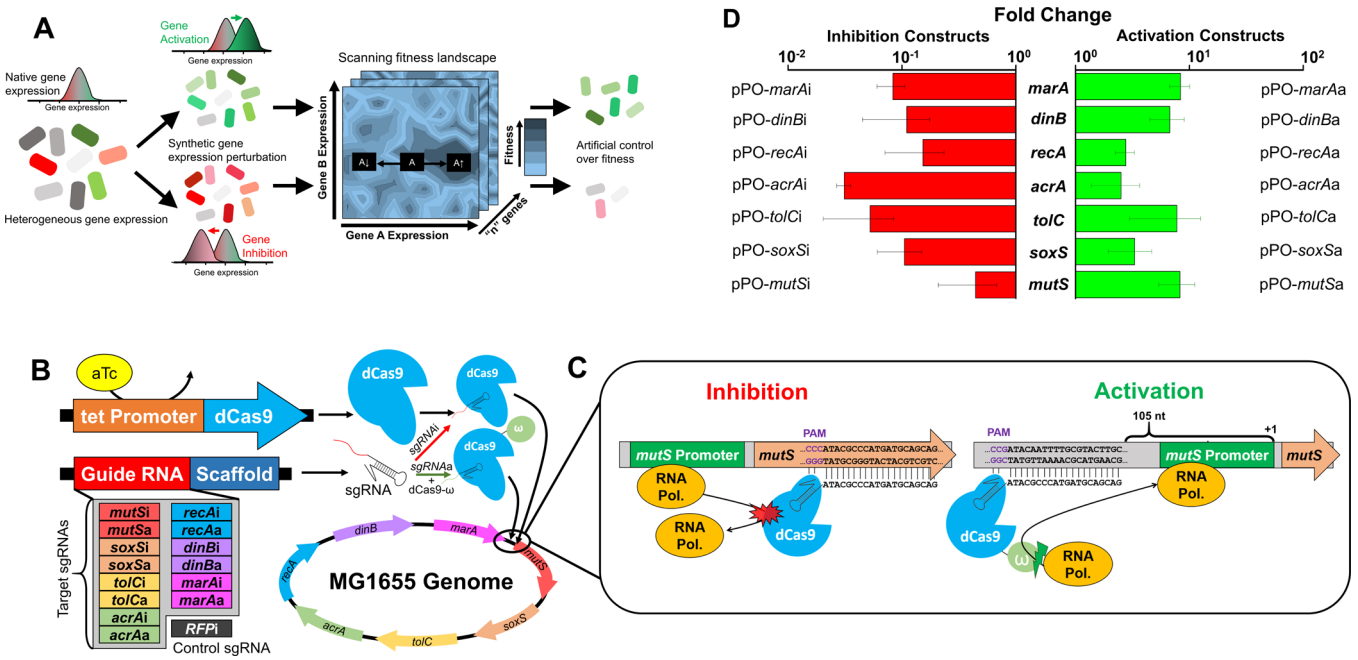

Figure 1. Design and characterization of synthetic CRISPR constructs perturbing gene expression. (A) Schematic demonstrating approach to engineer control over the theoretical bacterial fitness landscape.[45] By synthetically perturbing an individual gene's native expression by increasing (A↑) or decreasing (A↓) expression using synthetic CRISPR-Cas9 based genetic devices, unique fitness responses can be derived. This approach can further be applied to perturb multiple genes simultaneously to dynamically explore this adaptive landscape in *n* dimensions. (B) Schematic illustrating approach used to perturb gene expression in *E. coli*. Co-transformation of dCas9 (or dCas9-*ω*) plasmids with unique inhibition (or activation) sgRNA plasmids determined localization of proteins on the native *E. coli* MG1655 genome. These proteins combined *in vivo* with sgRNAs to individually perturb MG1655's expression of the seven genes shown. Note that constructs combined with the sgRNA targeting *rfp* did not bind to the genome, and thus served as controls. (C) Binding positions of *mutS* inhibition and activation constructs are shown. Inhibition constructs prevented RNAP read-through of the target's ORF, while activation constructs recruited RNAP to the promoter region by binding upstream of the +1 sequence. (D) RT-qPCR characterization of gene expression in MG1655 strains harboring dCas9 (inhibition constructs) or dCas9-*ω* (activation constructs) and sgRNA plasmids (pPO-*genei*/a), normalized to housekeeping gene *rrsA* and relative to wild-type MG1655. *genei* and *genea* indicate inhibition and activation respectively of the specific gene. Error bars represent standard deviation (s.d.) of biological triplicates.

knowledge is the first of its kind.[18] dCas9 and dCas9 constructs fused with the *ω*-subunit of RNA polymerase (dCas9-*ω*) have been shown to controllably inhibit[19] or activate[20] gene expression, respectively. When combined *in vivo* with small guide RNAs (sgRNAs), these devices exhibit highly specific and localized control over the transcription rates of individual genes. Moreover, these CRISPR devices are able to perturb expression of multiple genes simultaneously, thereby allowing for the investigation of combinatorial effects[19] of targeted gene control and the subsequent interactions this induces.

We chose to investigate seven stress-response genes, whose functions are outlined in Supplementary Table S1. These include the global transcriptional regulators *marA*, *soxS* and *recA*. MarA (multiple antibiotic resistance) activates expression of the *mar* operon to increase efflux activity, decrease porin expression, and regulate other biochemical processes to confer tolerance to solvents and drugs.[21] SoxS (superoxide stress response) shares 49% homology in binding sites with MarA, and regulates similar genes to promote antimicrobial tolerance.[22] RecA activates the SOS response, wherein DNA repair occurs and cell growth is arrested.[23] The remaining four genes we chose to examine were downstream genes of these global regulators: *mutS*, *dinB*, *acrA* and *tolC*. MutS functions in DNA mismatch repair pathways (thereby decreasing mutation rates),[24] while DinB acts as an error-prone polymerase lacking proofreading capacity (thereby increasing mutation rates).[25] Finally, TolC and AcrA work in tandem to construct an efflux pump to channel toxic materials outside of the cell.[26] We engineered CRISPR devices to systematically inhibit and activate the expression of these stress-response genes in *E. coli* during short-term (72 h) exposure to various stress conditions, including antibiotics (tetracycline and rifampicin), disinfectants (bleach and hydrogen peroxide) and glucose limitation. We monitored the resulting growth and fitness impacts during the early stages of adaptation, as well as the epistatic interactions induced by simultaneous gene perturbation.

Corroborating our hypothesis, we observe that CRISPR-Cas9 based synthetic devices enable small perturbations in gene expression that are sufficient to significantly influence native bacterial adaptive responses to stress by altering growth rates, lag times, and overall fitness. We show that these impacts are reversible upon stress removal, indicating their nongenetic nature. We demonstrate that simultaneous perturbations predominately induce negative epistasis, extending mutation-based epistasis concepts to the gene expression landscape. This work builds upon landmark gene knockout,[27] plasmid over-expression,[28] network rewiring[29] and long-term evolution[30] studies by outlining a novel synthetic biology approach for engineering control over bacterial adaptation via exogenously regulating gene expression profiles. Our study also helps to elucidate the early adaptive response preceding genome modifications, and serves as a paradigm shift in the field of antibiotic resistance research away from investigating downstream adaptations and toward pathways bacteria utilize for adaptation.

DOI: 10.1021/acssynbio.6b00050
ACS Synth. Biol. XXXX, XXX, XXX−XXX

A

Category	Stress	Concentration
Starvation	Glucose limitation	0.4% (vol/vol)
Antibiotic	Rifampicin	10.0 ng/μL
Antibiotic	Tetracycline	1.0 ng/μL
Disinfectant	Sodium Hypochlorite (bleach)	37.3 mM*
Disinfectant	Hydrogen peroxide	0.3 mM*

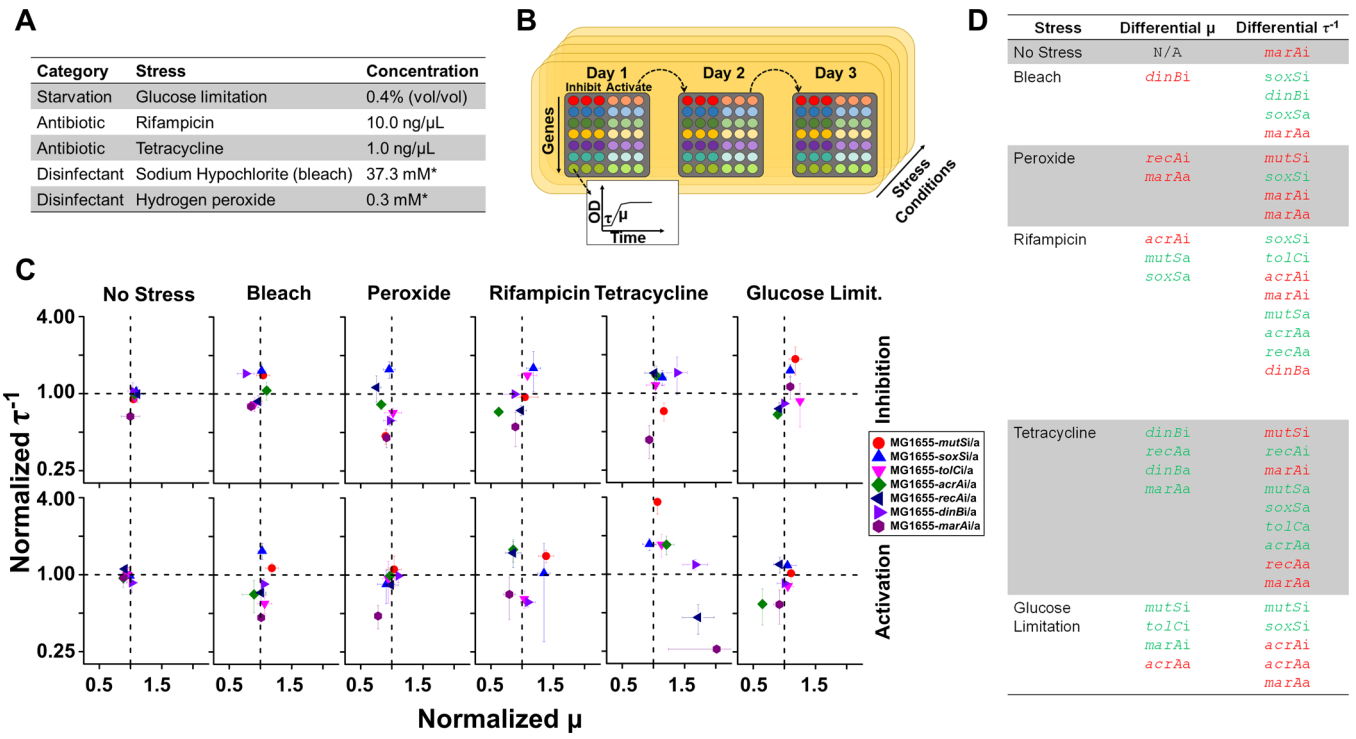

D

Stress	Differential μ	Differential τ^{-1}
No Stress	N/A	marAi
Bleach	dinBi	soxSi dinBi soxSa marAa
Peroxide	recAi marAa	mutSi soxSi marAi marAa
Rifampicin	acrAi mutSa soxSa	soxSi tolCi acrAi marAi mutSa acrAa recAa dinBa
Tetracycline	dinBi recAa dinBa marAa	mutSi recAi marAi mutSa soxSa tolCa acrAa recAa marAa
Glucose Limitation	mutSi tolCi marAi acrAa	mutSi soxSi acrAi acrAa marAa

Figure 2. Gene perturbation during stress exposure induces altered growth characteristics. (A) Starting sub-MIC levels of toxins and nutrients for the various stress conditions. (B) Experimental design of stress exposure while perturbing gene expression. Gene perturbation strains were exposed to individual stress conditions with serial dilution into fresh media after 24 h exposure. OD was measured to determine τ and μ on each day. (C) Comparison of μ_{norm} and $\tau^{-1}{}_{norm}$ averaged over 3 days, normalized to MG1655-Control. Deviations from intersecting dotted lines (control) indicate impacts on growth characteristics induced by perturbing gene expression with respect to MG1655-Control. The top row shows results from inhibition strains, while the bottom shows results from activation strains. Note, the *y*-axis uses Log_2 scaling. (D) Compiled list of results that were statistically significant at $P < 0.05$. Improvements in growth characteristics (μ_{norm} and $\tau^{-1}{}_{norm}$) are denoted in green; impairments are denoted in red. *P*-values were calculated using one-way ANOVA with Tukey *posthoc* HSD test (using $\alpha < 0.05$). Error bars represent s.d. of biological triplicates.

RESULTS

Design and Characterization of Single Target Gene Perturbation Devices. To accomplish controlled gene expression perturbation, we designed and synthesized (see Methods) a set of 14 Type II CRISPR sgRNA plasmid constructs to inhibit or activate transcription of seven stress-response genes in *E. coli*, chosen for their known influence on adaptation[21−26] (Figure 1B and Supplementary Figure S1). The sgRNA constructs were named pPO-*gene*i or pPO-*gene*a for inhibition and activation respectively of each given gene (Supplementary Table S2), and were co-transformed alongside a separate plasmid containing anhydrotetracycline (aTc) inducible dCas9 or dCas9-ω into *E. coli* strain MG1655. This produced 14 unique experimental perturbation strains, designated MG1655-*gene*i or MG1655-*gene*a. Two control strains harboring dCas9 or dCas9-ω plasmids, as well as the control sgRNA construct sgRNA-RFPi (targeting the *rfp* coding sequence not present in MG1655) were also created (Supplementary Table S3). All sgRNAs utilized common promoter and scaffolding elements, but differed in their unique 20 nucleotide (nt) sequence-specific DNA-binding domain. Inhibition and activation sgRNAs were coupled *in vivo* with dCas9 or dCas9-ω respectively to form the final protein-RNA hybrid construct with inherent DNA-binding affinity for the 20 nt sequences of each sgRNA, allowing for specific control of gene expression (Figure 1C). Activation sgRNAs targeting ≈80−110 nt upstream of the +1 transcription start site of each gene provided optimal spacing for RNA polymerase to bind to the promoter and increase gene expression.[20] Inhibition sgRNAs targeted within the first ≈50 nt of the genes' open reading frame (ORF) to inhibit transcriptional read-through via a roadblock mechanism.[19] Each CRISPR target sequence was flanked by an "NGG" Protospacer-Adjacent-Motif (PAM) on the 3′end for proper binding of the protein-RNA complex with the target DNA.[19] The impact of a subset of these constructs on neighboring genes' expression was quantified and was found to be either absent or minimal (Supplementary Figure S2). It is expected that perturbing each of these genes may induce changes in expression of downstream genes as governed by the connections through respective gene regulatory networks within *E. coli*.

The ability of bacteria to evolve resistance depends on the accessibility of higher-fitness states within a hypothetical "adaptive landscape", which can be visualized as a multidimensional space comprised of the variable expression states of *n*-by-*n* genes (analogous to similar adaptive landscapes based on gene mutations)[31−33] (Figure 1A). Cloning our library of synthetic CRISPR devices into MG1655 enabled us to engineer a set of strains in which this adaptive landscape was perturbed. By inhibiting or activating individual genes, these strains enabled exploration of the impact that gene expression has on stress response. An advantage of using CRISPR devices is that this approach does not directly modify the wild-type genome, allowing for investigation of adaptive pathways in their natural state without the need to create a unique genome for each gene studied as done in canonical gene knockout studies, and thereby provides a unique insight.

DOI: 10.1021/acssynbio.6b00050
ACS Synth. Biol. XXXX, XXX, XXX−XXX

To measure the effects of gene perturbation, we utilized RT-qPCR to quantify the gene expression of each of these strains relative to wild-type MG1655. Our results indicate that the strains' expression profiles were indeed perturbed as intended, with a range of 32-fold reduction to 8-fold increase in gene expression (Figure 1D). Optimization of expression perturbation was influenced by native gene orientation; for instance, binding of dCas9-ω upstream of the +1 *soxS* transcription start site necessitated overlap with the ORF of *soxR*, an activator of *soxS*. Growth tests were also performed to analyze the viability of these strains. No loss of viability that is not intrinsic to growth with two plasmids was observed (Supplementary Figure S3). Since MG1655-*rfp*i and MG1655-*rfp*a strains demonstrated similar growth characteristics, we used MG1655-*rfp*a as the control strain in subsequent stress-exposure experiments (referred to hereafter as the MG1655-Control).

Perturbation of Gene Expression Influences Bacterial Growth Characteristics during Stress Exposure. We sought to examine the growth of strains harboring the CRISPR constructs under various environmental stresses to which infectious bacteria are commonly exposed, to determine whether artificial perturbation of gene expression enabled control over bacterial growth (and thus adaptive potential). To achieve this, five stress conditions were selected representing oxidizing agents (household bleach[34] and hydrogen peroxide[35]), antibiotics (tetracycline[36] and rifampicin[37]), and nutrient limitation (M9 minimal media supplemented with 0.4% glucose). The Minimum Inhibitory Concentration (MIC) was determined using MG1655-Control to estimate the appropriate starting concentrations for growth under each stress condition (Supplementary Figure S4). The sub-MIC levels were used as starting points for stress exposure experiments (Figure 2A, see Methods). We exposed *E. coli* strains harboring the CRISPR constructs to each stress over a course of 72 h (Figure 2B), transferring biological triplicates every 24 h into fresh media supplemented with aTc and antibiotics to maintain plasmid selection (see Methods). During this time, optical densities (ODs) were monitored to track changes in growth rate (μ) and inverse lag phase (τ^{-1}) on each day of the experiment (SI Extended Data Set). These data was normalized to MG1655-Control by dividing μ and τ^{-1} by the average performance of biological triplicates of MG1655-Control from the experimental day (creating μ_{norm} and ${\tau^{-1}}_{norm}$). Normalized data was averaged over three experimental days. Adapting bacterial populations have been shown to exhibit significant heterogeneity in growth rates[38] and lag times,[39] and thus these serve as useful metrics to quantitatively compare adaptive trends between strains. We chose to keep lag times in their reciprocal format, as larger lag times (smaller inverse lag time, ${\tau^{-1}}_{norm} < 1.0$) indicate that cells are stalling longer before growth and are thus considered detrimental. We found that the overall correlation between ${\tau^{-1}}_{norm}$ and μ_{norm} was negligible (Pearson's correlation coefficient, $r = 0.09$, F-value =0.69), indicating that these independently provided insight into changes in growth caused by gene perturbation (Supplementary Figure S5).

A two-dimensional analysis of normalized τ^{-1} and μ revealed greater diversity during stress exposure than was observed under no stress (Figure 2C). From these data, 14 of the 84 growth rates (14 perturbation constructs ×6 growth conditions) and 31 of the 84 lag times demonstrated statistically significant shifts from MG1655-Control (Figure 2D). With the exception of MG1655-*marA*i, none of these shifts occurred in the absence of stress exposure, indicating that perturbations of these genes predominantly did not inherently diminish or enhance bacterial growth in absence of stress. Calculating the sum of distances (D_i and D_a for inhibition and activation constructs respectively) from the expected performance under no perturbation ($\mu_{norm} = {\tau^{-1}}_{norm} = 1.0$) revealed relatively minor changes under no stress ($D_i = 0.87$, $D_a = 0.63$) than under the exposure to bleach ($D_i = 2.11$, $D_a = 2.46$), peroxide ($D_i = 2.84$, $D_a = 1.24$), glucose limitation ($D_i = 2.60$, $D_a = 1.82$), and especially the antibiotics rifampicin ($D_i = 2.40$, $D_a = 3.12$) and tetracycline ($D_i = 2.81$, $D_a = 7.70$). Notably, these results indicate that shifts in growth characteristics from the control strain (deviations from the dotted lines) increased significantly during the presence of stress, demonstrating the potential that synthetically engineered gene perturbations have to artificially control the adaptive response.

Performance of perturbation strains during exposure to oxidizing agents resulted in reduced growth rates than was observed under other conditions, accounting for three of the five statistically lower μ phenotypes. Under bleach exposure, MG1655-*dinB*i demonstrated reduced μ_{norm} (0.76 ± 0.14, $P = 0.020$) and increased ${\tau^{-1}}_{norm}$ (1.44 ± 0.05, $P = 0.016$), while under peroxide exposure MG1655-*marA*a demonstrated both reduced μ_{norm} (0.78 ± 0.04, $P = 0.039$) and ${\tau^{-1}}_{norm}$ (0.48 ± 0.10, $P = 0.048$). Lag times in particular were impacted by gene perturbations during exposure to antibiotics, affecting 8 of 14 strains grown in rifampicin and 9 of 14 strains grown in tetracycline. Under rifampicin stress, MG1655-*acrA*i demonstrated impaired growth characteristics ($\mu_{norm} = 0.62 \pm 0.07$, $P = 0.038$ and ${\tau^{-1}}_{norm} = 0.72 \pm 0.05$, $P = 0.021$), while MG1655-*mutS*a showed opposite effects ($\mu_{norm} = 1.38 \pm 0.12$, $P = 0.044$ and ${\tau^{-1}}_{norm} = 1.40 \pm 0.16$, $P = 0.031$). Under tetracycline stress, both MG1655-*recA*a and MG1655-*marA*a demonstrated improved growth rates ($\mu_{norm} = 1.72 \pm 0.26$, $P = 0.022$ and $\mu_{norm} = 2.01 \pm 0.77$, $P = 0.0010$ respectively) and extended lag times (${\tau^{-1}}_{norm} = 0.46 \pm 0.12$, $P = 0.022$ and ${\tau^{-1}}_{norm} = 0.26 \pm 0.02$, $P = 0.0077$ respectively). Under glucose limitation, MG1655-*soxS*i showed improved growth characteristics (${\tau^{-1}}_{norm} = 1.52 \pm 0.19$, $P = 0.012$), while MG1655-*acrA*a demonstrated the opposite effect ($\mu_{norm} = 0.65 \pm 0.06$, $P = 0.0014$ and ${\tau^{-1}}_{norm} = 0.59 \pm 0.19$, $P = 0.037$). Overall, these results corroborate the hypothesis that small artificial perturbations in gene expression during stress exposure significantly influence native bacterial adaptive responses.

Notably, gene perturbation under each stress condition produced unique results, indicating a complex underlying cellular response network unique to each stress. Furthermore, inhibition and activation of the same gene did not necessarily induce antagonistic effects under the same stress. For example, inhibition of *dinB* decreased μ during bleach exposure, but both inhibition and activation of *dinB* increased μ in tetracycline. Another intriguing result we observed was that both MG1655-*marA*i and MG1655-*marA*a demonstrated significant increases in τ (under all stresses besides bleach and glucose limitation for MG1655-*marA*i and under all stresses but rifampicin for MG1655-*marA*a). This was most pronounced under tetracycline exposure (${\tau^{-1}}_{norm} = 0.43 \pm 0.12$, $P = 0.0029$ and ${\tau^{-1}}_{norm} = 0.26 \pm 0.02$, $P = 0.011$ for inhibition and activation, respectively). A correlation between overexpression of *marA* and an increase in lag time has previously been reported.[40] Conversely, MG1655-*soxS*i demonstrated reduced τ under all stresses (with the exception of tetracycline stress, where $P = 0.084$, all were statistically significant), while MG1655-*soxS*a

DOI: 10.1021/acssynbio.6b00050
ACS Synth. Biol. XXXX, XXX, XXX−XXX

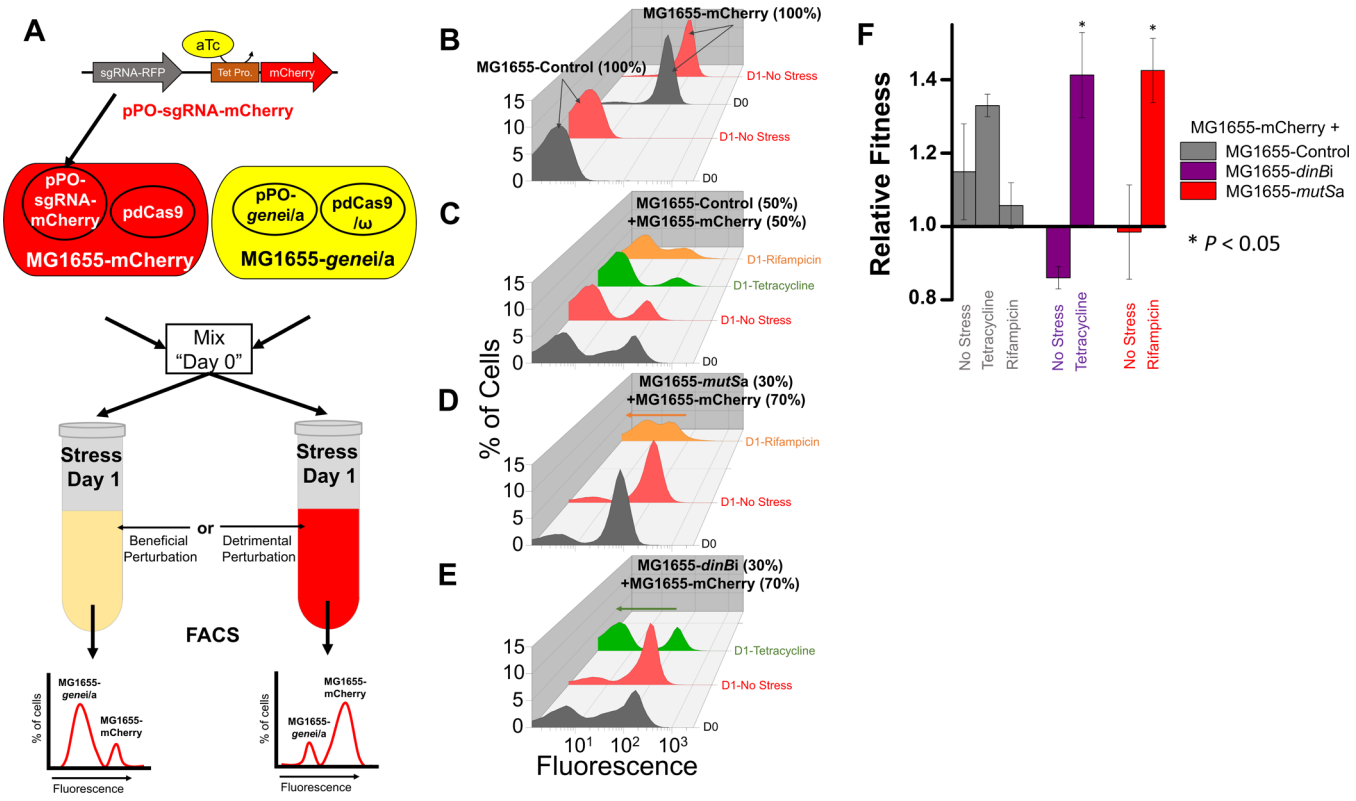

Figure 3. Competition assays reveal changes in fitness resulting from gene perturbations. (A) The protein mCherry, which fluoresces red, was cloned onto the sgRNA-RFPi plasmid and co-transformed into MG1655 with pdCas9 to create a fluorescent strain with basal gene expression. This strain could be distinguished from experimental MG1655 strains with perturbed gene expression via its greater fluorescence, as determined by FACS. (B–E) Representative set of FACS data from competition experiment. All day 1 populations (D1) were inoculated from the same day 0 population (D0) in their respective graphs. (B) FACS analysis of pure MG1655-Control and MG1655-mCherry strains before (D0) and after (D1) 1 day of growth under no stress. (C) Control FACS analysis experiment results. MG1655-Control and MG1655-mCherry were mixed at equal starting ODs, and grown for 1 day under no stress (red), tetracycline (green) or rifampicin stress (orange), showing no discernible selection for either strain. (D) FACS analysis revealed selection of MG1655-*mutS*a when competed against MG1655-mCherry under rifampicin stress, despite having a lower starting concentration (30% by OD). (E) Likewise, FACS analysis revealed selection of MG1655-*dinB*i when competed against MG1655-mCherry under tetracycline stress, despite having a lower staring concentration (30% by OD). (F) Relative fitness levels of each strain in relation to the MG1655-mCherry strain, showing significant changes only during stress exposure across biological triplicates. *P*-values were calculated using a two-tailed type II *t*-test, and are in relation to the no stress condition for each competition experiment. Error bars represent s.d. of biological triplicates.

also demonstrated reduced τ under bleach and tetracycline stress. Increased (or decreased) τ could indicate activation (or suppression) of persistence, which bacteria are known to employ as a survival strategy during sudden stress exposure.[39] This serves as an interesting avenue for future research into the relation between *marA* and *soxS* gene expression perturbation and the induction of persistence.

Competition Assay Corroborates Fitness Impacts of Gene Perturbation. We hypothesized that if growth characteristics improved (or diminished) as a result of induced gene perturbation, then such perturbations should also provide a competitive advantage (or disadvantage) impacting bacterial fitness. To test this hypothesis, we performed competition assays between a select subset of MG1655-*genei*/a CRISPR perturbation strains based on their phenotypic performances under stress, as well as a new control strain MG1655-mCherry. The MG1655-mCherry strain was analogous to MG1655-Control, but also included the coding sequence for mCherry on the sgRNA-RFPi plasmid. By mixing MG1655-mCherry with strains of interest, we could determine the relative fitness impacts of gene perturbation during stress exposure utilizing flow-activated cell sorting (FACS) (Figure 3A). A mixture of the two strains grown under stress was analyzed before (D0) and after 1 day (D1) of stress exposure. The fluorescence of the total population was used to determine the relative ratios of the control strain with basal levels of gene expression (which fluoresced red due to the presence of mCherry) to the strain with perturbed gene expression (which did not fluoresce due to the absence of mCherry). Pure (100%) MG1655-mCherry and MG1655-Control populations distributed into two distinct fluorescence intervals both on D0 and D1 (Figure 3B). When mixed equally (50% by OD), statistically significant selection for either MG1655-mCherry or MG1655-Control was not observed after 1 day of exposure to tetracycline or rifampicin when compared to no stress condition (Figure 3C).

To demonstrate that the MG1655-*genei*/a strains impacted bacterial fitness during stress exposure, we utilized this competition assay approach to compare the fitness of MG1655-*mutS*a under rifampicin and MG1655-*dinB*i under tetracycline against MG1655-mCherry. These strains were selected for their measured impacts on μ shown in Figure 2. Because these strains improved μ in rifampicin or tetracycline, we chose to reduce their starting concentration (30%) relative to MG1655-mCherry (70%) on D0. As expected, activation of *mutS* and inhibition of *dinB* caused a shift in the relative population density away from MG1655-mCherry and toward

DOI: 10.1021/acssynbio.6b00050
ACS Synth. Biol. XXXX, XXX, XXX–XXX

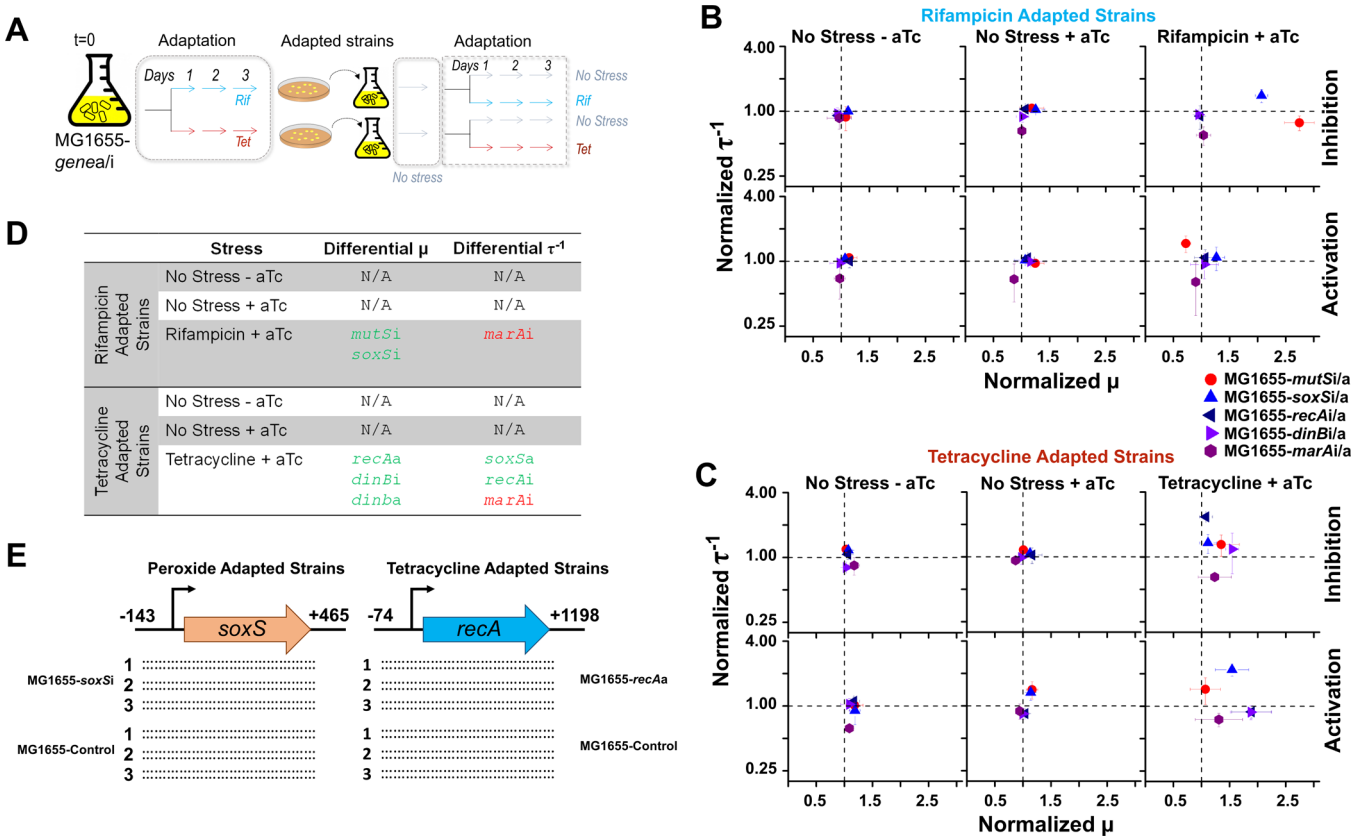

Figure 4. Evidence of phenotypic reversibility of adapted strains. (A) Schematic illustrating approach to investigate reversibility of phenotypic changes observed during growth under stress. Strains collected after 72 h of stress exposure were plated, grown for 24 h under no stress, and exposed to either no stress (with and without aTc induction) or the initial stress they were exposed to. (B) Strains exposed to rifampicin stress were collected and grown for another 3 days under either no stress or rifampicin exposure. Perturbation strains behaved similarly to MG1655-Control once returned to no stress, but maintained their unique phenotypes under rifampicin exposure. Error bars represent s.d. of biological triplicates. (C) A similar phenomenon was observed by strains which were exposed to tetracycline stress, collected, and grown for another 3 days under either no stress or tetracycline exposure. (D) Statically significant deviations in μ and τ^{-1} of rifampicin and tetracycline adapted strains after re-exposure to stress, using a one-way ANOVA with Tukey *posthoc* HSD test (using $\alpha < 0.05$). (E) After exposure to peroxide (MG1655-*soxS*i and MG1655-Control) and tetracycline (MG1655-*recA*a and MG1655-Control), biological duplicates of each biological triplicate were sequenced around the genetic region where synthetic perturbation constructs targeted. Sequenced regions are indicated with respect to the +1 of the promoter. No mutations were observed in any of the 24 strains. Dots indicate change with respect to the wild-type.

MG1655-*mutS*a (Figure 3D) or MG1655-*dinB*i (Figure 3E) after 1 day of exposure to their respective stresses, but not during the absence of stress. The same trend demonstrated in Figure 3D was observed during competition of MG1655-*mutS*a against MG1655-mCherry using equal starting concentrations in two different growth media (LB and M9 minimal media), indicating that these results were independent of the starting competition ratio as well as the media chosen (Supplementary Figure S6). These results were reproduced across biological triplicates, demonstrating statistically significant improvements in fitness under stress exposure (Figure 3F). We also observed the opposite effect; when MG1655-*acrA*i (70%), which exhibited reduced μ under rifampicin stress (Figure 2C−D), was competed against MG1655-mCherry (30%), the latter was selected for despite having a lower starting concentration (30%) when exposed to rifampicin stress (Supplementary Figure S7).

Furthermore, this method was utilized to estimate the fitness of each strain relative to MG1655-mCherry (Figure 3F). FACS data was used to estimate the proportion of fluorescent and nonfluorescent cells before and after 1 day of stress exposure, from which Malthusian (m) parameters were calculated for each of the two competing strains.[41] The m ratios were used to calculate relative fitness (see Methods) from three biological replicates. The relative fitness of MG1655-Control was not statistically different between antibiotic exposure and no stress exposure conditions. However, the relative fitness of MG1655-*dinB*i was greater under tetracycline stress (1.41 ± 0.11, P = 0.00007), while MG1655-*mutS*a was greater under rifampicin stress (1.43 ± 0.09, P = 0.02) demonstrating that these strains were selected for over MG1655-mCherry only during stress exposure. Overall, these results corroborate the measured fitness impacts on growth characteristics as shown in Figure 2C−D.

Phenotypic Reversibility and Evidence of Nongenetic Impact of Transcriptional Perturbation. We next tested the reversibility of the phenotypic deviations of these experimental strains from MG1655-Control; that is, whether or not the CRISPR-perturbed strains demonstrated similar growth characteristics as the control upon removal of stress. Such reversion under no stress would highlight the nongenetic nature of the observed changes in growth characteristics and fitness. We performed such analysis on a subset of biological triplicates collected at the end of 3 days of exposure to tetracycline and rifampicin stress (Figure 4A). These strains were grown for 1 day in the absence of stress and aTc induction. Afterward, each

DOI: 10.1021/acssynbio.6b00050
ACS Synth. Biol. XXXX, XXX, XXX−XXX

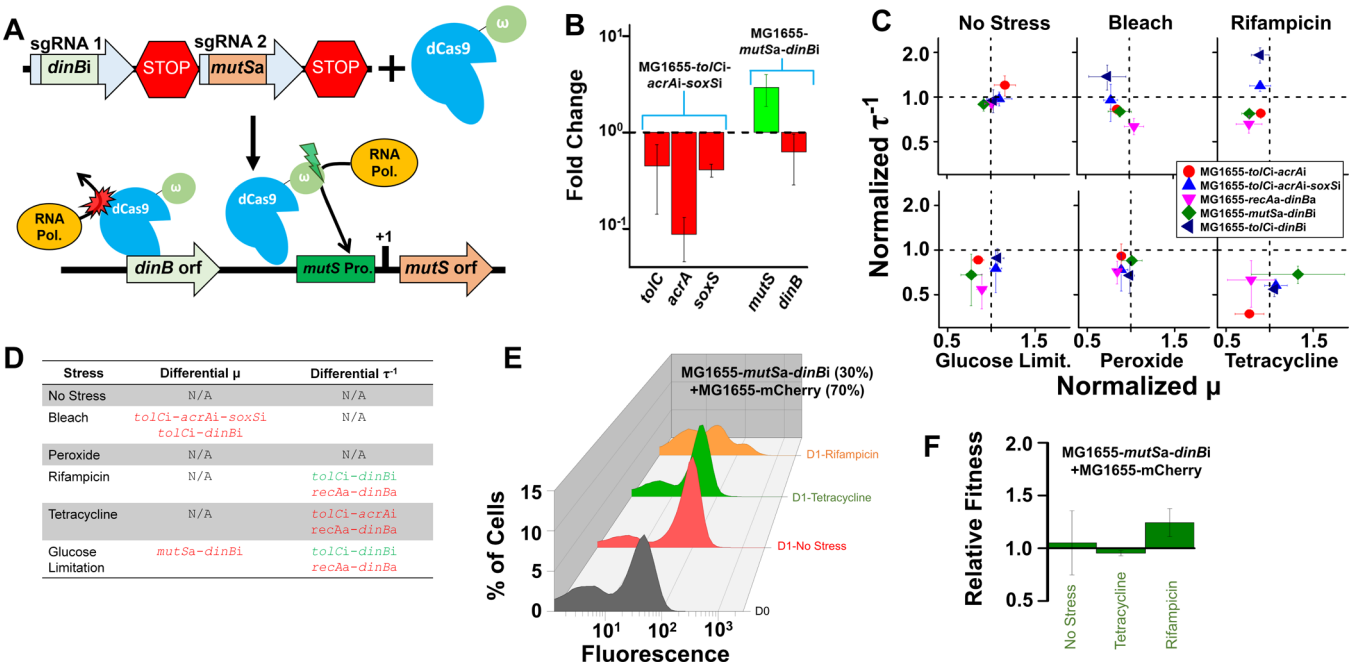

Stress	Differential μ	Differential τ⁻¹
No Stress	N/A	N/A
Bleach	tolCi-acrAi-soxSi tolCi-dinBi	N/A
Peroxide	N/A	N/A
Rifampicin	N/A	tolCi-dinBi recAa-dinBa
Tetracycline	N/A	tolCi-acrAi recAa-dinBa
Glucose Limitation	mutSa-dinBi	tolCi-dinBi recAa-dinBa

Figure 5. Utilization of CRISPR constructs to simultaneously perturb expression of multiple genes. (A) Strategy for perturbing multiple genes simultaneously involved cloning tandem targets into sgRNA constructs, which were transcribed individually to guide dCas9 or dCas9-ω (as demonstrated by constructs harbored by MG1655-*mutSa*-*dinBi*). (B) RT-qPCR characterization of gene expression in strains MG1655-*tolCi*-*acrAi*-*soxSi* and MG1655-*mutSa*-*dinBi* relative to wild-type MG1655, normalized to the housekeeping gene *rrsA*, revealing constructs simultaneously perturbed multiple genes' expression states as intended. (C) Impact of constructs on growth characteristics under various stress conditions, relative to MG1655-Control (dotted lines). (D) Compiled list of growth characteristics that were statistically significant at $P < 0.05$. Improvements in growth characteristics (normalized values greater than 1.0) are denoted in green; impairments are denoted in red. (E) Representative set of FACS data from competition of MG1655-*mutSa*-*dinBi* against MG1655-mCherry. Cells were mixed such that MG1655-*mutSa*-*dinBi* constituted 30% of the total starting OD. Unlike MG1655-*mutSa* or MG1655-*dinBi*, this strain was not selected for under tetracycline or rifampicin stress. (F) Fitness of MG1655-*mutSa*-*dinBi* relative to MG1655-mCherry, in which fitness under stress was not shown to be statistically different than fitness under no stress across biological triplicates. *P*-values were calculated using one-way ANOVA with Tukey *posthoc* HSD test (using $\alpha < 0.05$). Error bars represent s.d. of biological triplicates.

strain was re-exposed to the three day adaptation experiment in the absence of stress both with and without aTc, or the same initial stress and aTc. For rifampicin adapted strains, we observed a return to the wild-type phenotype in no stress both in the absence ($D_i = 0.60$, $D_a = 0.96$) and presence ($D_i = 0.99$, $D_a = 0.75$) of aTc induction of gene perturbation (Figure 4B). A similar phenomenon was observed in tetracycline adapted strains under no stress in the absence ($D_i = 0.90$, $D_a = 1.08$) and presence ($D_i = 1.24$, $D_a = 0.66$) of aTc (Figure 4C). Together, these data indicate that the phenotypic effects of gene expression perturbations were reversible upon stress removal, suggesting their nongenetic nature.

When stress was maintained, perturbation strains continued to demonstrate deviations in μ and τ^{-1} under rifampicin exposure ($D_i = 3.49$, $D_a = 1.38$) as well as tetracycline exposure ($D_i = 3.18$, $D_a = 3.93$). A majority of strains exhibited similar phenotypes during both the first and second round of rifampicin exposure. MG1655-*marA*i again demonstrated a reduced ${\tau^{-1}}_{norm}$ (0.66 ± 0.08, $P = 0.038$). The previously identified lag time impacts of MG1655-*recA*i, MG1655-*recA*a and MG1655-*dinB*a became less pronounced. Two new phenotypes were observed only during the second round of rifampicin exposure: MG1655-*mutS*i ${\mu_{norm}}$ (2.74 ± 0.27, $P = 6.9 \times 10^{-8}$) and MG1655-*soxS*i ${\mu_{norm}}$ (2.07 ± 0.11, $P = 1.2 \times 10^{-5}$). The difference in phenotypes between the first and second rounds of adaptation could be explained by an altered epigenetic state over an extended period of adaptation.

Under the second round of tetracycline exposure, no such new phenotypes were observed. Six previous statistically significant results remained; MG1655-*recA*a, MG1655-*dinB*i and MG1655-*dinB*a exhibited increased ${\mu_{norm}}$ (1.89 ± 0.35, $P = 0.041$, 1.55 ± 0.11, $P = 0.0040$ and 1.88 ± 0.36, $P = 0.042$), MG1655-*soxS*a and MG1655-*recA*i exhibited increased ${\tau^{-1}}_{norm}$ (2.18 ± 0.35, $P = 0.0084$ and 2.35 ± 0.08, $P = 0.0019$ respectively), and MG1655-*marA*i exhibited decreased ${\tau^{-1}}_{norm}$ (0.65 ± 0.03, $P = 0.042$).

We next sequenced the experimental strains for mutations. Both MG1655-Control and gene perturbation strains received the same basal level of selection pressure to accumulate alterations at the genomic level. However, it is theoretically possible that CRISPR perturbations could have artificially induced mutations in their genomic targets to circumvent the synthetically induced gene expression changes, undermining the observed phenotypic changes in perturbation strains. To test for this possibility, we chose to sequence the genes directly influenced by perturbation in a subset of our strains (Figure 4E). We sequenced the region of *soxS* in MG1655-*soxS*i after exposure to peroxide stress, as well as the region of *recA* in MG1655-*recA*a after exposure to tetracycline stress, since these gene perturbations showed significant impact on μ and τ^{-1} respectively. We also sequenced MG1655-Control after exposure to each condition, to account for any mutations not influenced by gene perturbation. Sequencing of six biological replicates per strain provided no evidence of mutations, indicating that these perturbations likely did not induce

DOI: 10.1021/acssynbio.6b00050
ACS Synth. Biol. XXXX, XXX, XXX−XXX

mutations in the genomic regions they targeted. However, these results do not discount the possibility of unique mutations arising in experimental strains and not in MG1655-Control or vice versa. It is expected that the gene perturbations could have influenced other genomic regions to mutate during stress exposure.

In order to characterize the consequence of gene perturbations on mutation rates across the genome, we performed a mutation fluctuation assay on a subset of strains: MG1655-Control, MG1655-*mutS*i, MG1655-*mutS*a, MG1655-*soxS*i, MG1655-*soxS*a, MG1655-*dinB*i, MG1655-*dinB*a and MG1655-*mutS*i-*dinB*a (Supplementary Figure S8). Our results indicated no significant difference in mutation rates with the notable exception of MG1655-*soxS*a, which was shown to have a significantly increased mutation rate over MG1655-Control in the absence of stress (1.6×10^{-8} *versus* 5.1×10^{-10} respectively). One possibility for the increased mutation rates of MG1655-*soxS*a is an increased expression of Endonuclease IV gene *nfo*, one of the genes regulated by SoxS.[42] In general, however, these data show that gene perturbation predominantly appears to not significantly influence mutation rates in the absence of stress.

Together, these data point toward the fact that the observed changes in growth and fitness phenotypes are mainly an effect induced by the CRISPR devices, and are unlikely to be caused by independent genetic changes that arose in absence of CRISPR perturbation influence.

Design and Characterization of Strains Perturbing Multiple Targets Simultaneously. We next explored the combinatorial effects of up-regulating or down-regulating multiple genes simultaneously with CRISPR constructs. In principle, combining several independent sgRNA targets into one construct allows for controlled perturbation of multiple genes' expression patterns, as has recently been demonstrated.[43] This provides a powerful tool to tune expression of multiple genes (either increase or decrease expression) without the need to use multiple artificial promoters that require to be integrated into the genome. We demonstrated simultaneous induction of synthetic gene perturbations using a modified cloning approach that introduced tandem independent sgRNAs onto one plasmid to combine *in vivo* with dCas9 or dCas9-ω (Supplementary Figure S9). We designed three constructs in which the perturbed genes had known regulatory interactions: MG1655-*tolC*i-*acrA*i (which inhibited the AcrAB-TolC multidrug efflux pump), MG1655-*mutS*a-*dinB*i (which activated expression of a mismatch-repair protein and decreased expression of an error-prone polymerase, thereby likely decreasing mutation rates), and MG1655-*recA*a-*dinB*a (which increased expression of *DinB* both directly and indirectly by increasing expression of its upstream up-regulator *RecA*). We designed a fourth construct, MG1655-*tolC*i-*acrA*i-*soxS*i, which inhibited three genes simultaneously which showed similar impacts on growth characteristics in Figure 2C−D (MG1655-*tolC*i and MG1655-*soxS*i increased μ under glucose limitation and τ under rifampicin exposure, while MG1655-*acrA*i and MG1655-*soxS*i increased τ under tetracycline exposure). Finally, we designed a fifth construct, MG1655-*tolC*i-*dinB*i, which perturbed two genes in separately regulated pathways and have not been shown to produce similar impacts on growth characteristics under the same stress condition.

Strains engineered to only exhibit inhibited gene expression utilized dCas9, while strains engineered to exhibit activation of one or more genes utilized dCas9-ω. Notably, strain MG1655-*mutS*a-*dinB*i demonstrates that simultaneous activation and inhibition of gene expression is possible through the use of dCas9-ω (Figure 5A). Previous work using a dCas9-VP64 eukaryotic transcriptional activator validated that CRISPR activation constructs can reliably inhibit gene expression when targeted to areas downstream of the promoter sequence.[44] We utilized RT-qPCR to verify that MG1655-*mutS*a-*dinB*i (as well as MG1655-*tolC*i-*acrA*i-*soxS*i) perturbed gene expression as intended (Figure 5B). Growth for 72 h under stress was repeated for strains harboring these multi-target synthetic constructs.

The effects of modulating gene expression on growth characteristics were quantified, again normalizing data against the MG1655-Control strain grown alongside the multitarget strains (Figure 5C and SI Extended Data Set). We found 3 of 30 measured μ (5 perturbation constructs ×6 growth conditions) and 6 of 30 measured τ^{-1} were significantly impacted by simultaneous gene perturbations. Surprisingly, 7 of the 9 statistically different growth characteristics measured by these strains were detrimental, *i.e.*, decreased μ_{norm} or ${\tau^{-1}}_{norm}$. The only two improvements were exhibited by a higher ${\tau^{-1}}_{norm}$ of MG1655-*tolC*i-*dinB*i under rifampicin stress and glucose limitation (Figure 5D). Conversely, MG1655-*recA*a-*dinB*a demonstrated reduced ${\tau^{-1}}_{norm}$ under three different conditions: rifampicin stress (${\tau^{-1}}_{norm} = 0.66 \pm 0.09$, $P = 0.0064$), tetracycline stress (${\tau^{-1}}_{norm} = 0.63 \pm 0.22$, $P = 0.0030$) and glucose limitation (${\tau^{-1}}_{norm} = 0.54 \pm 0.14$, $P = 0.0081$). Interestingly, the perturbation of *recA*a and *dinB*a alone had reciprocal impacts under rifampicin and tetracycline stress, and no significant impact under glucose limitation. These results indicated that the growth of strains with simultaneously perturbed genes was diminished in relation to single target strains.

As before with single gene perturbation, we employed competition assays between MG1655-*mutS*a-*dinB*i and MG1655-mCherrry to further analyze the fitness impacts induced by simultaneous gene perturbation. We saw no selection for MG1655-*mutS*a-*dinB*i after 1 day of stress exposure in either rifampicin or tetracycline (Figure 5E). Competition was also performed between MG1655-mCherry and MG1655-*tolC*i-*dinB*i, which did show a shift toward the latter population after rifampicin exposure as predicted by growth characteristic data (Supplementary Figure S10). Using Malthusian (m) parameters calculated from biological triplicates, there was no statistically significant difference between the relative fitness of MG1655-*mutS*a-*dinB*i under no stress and the relative fitness under either stress (Figure 5F). These data contrasts the improved fitness of MG1655-*mutS*a and MG1655-*dinB*i in rifampicin and tetracycline respectively that was previously observed (Figure 3D−F). This suggests that strains in which multiple genes are perturbed are less fit than would be expected based on results from single gene perturbation strains.

Simultaneous Gene Perturbation Predominantly Yields Negative Epistatic Interactions. We next examined the epistasis induced by simultaneous gene perturbation (recently characterized as "epigenetic" epistatic interactions[17]), given that a large number of strains harboring multiple gene targeting CRISPR constructs elicited a less-fit phenotype than predicted from the performance of strains harboring their single target constituents. To do so, we utilized a multiplicative model to calculate epistasis in both μ_{norm} and ${\tau^{-1}}_{norm}$ for each of the five strains with simultaneous gene perturbations. The expected growth rates (or inverse lag times)

DOI: 10.1021/acssynbio.6b00050
ACS Synth. Biol. XXXX, XXX, XXX−XXX

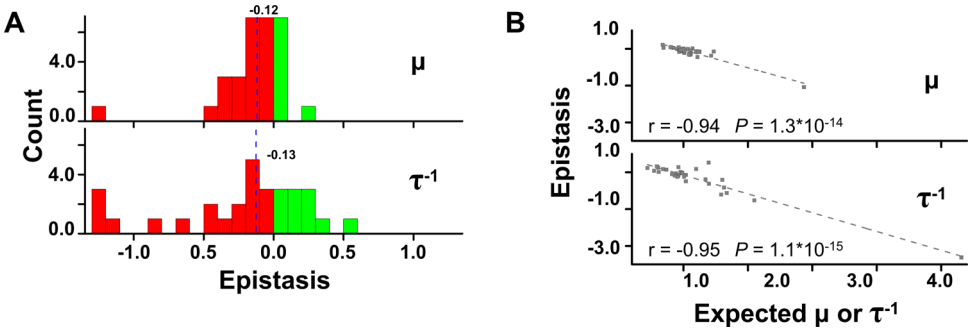

Figure 6. Induction of negative epistasis due to simultaneous gene perturbation. (A) Distribution of epistatic interactions on μ_{norm} and τ^{-1}_{norm} of five strains in which genes were simultaneously perturbed, over all six growth conditions. The distribution is skewed to the left, revealing the prevalence of negative epistasis resulting from simultaneous gene perturbation. Vertical blue lines indicate median values of epistasis. (B) A strong negative correlation was observed between the expected growth characteristic of the five strains and their measured epistatic interactions. Linear fits utilize epistasis data from all five strains under all six growth conditions.

of these strains were calculated by multiplying together the μ_{norm} (or τ^{-1}_{norm}) of each single gene perturbation strain from which they were created, and epistasis was calculated as the difference between these expected values and those that were measured (see Methods).

Epistasis in μ_{norm} and τ^{-1}_{norm} was quantified for each strain under each growth condition, and the distribution of epistasis was analyzed (Figure 6A). Indeed, we observed a distinct pervasiveness of negative epistasis resulting from simultaneous gene perturbation in both μ_{norm} (mean epistasis = -0.17 ± 0.14 [95% confidence interval], $P = 0.02$) and in τ^{-1}_{norm} (mean epistasis = -0.35 ± 0.33 [95% confidence interval], $P = 0.04$). A large majority of the data (73% of μ_{norm} epistasis and 63% of τ^{-1}_{norm} epistasis) falls into the category of negative epistasis, and both distributions are markedly skewed toward greater magnitudes of negative epistasis. These results help to explain the prevalence of diminished growth characteristics and fitness observed. The data also suggests that when two or more genes are perturbed from their basal expression levels, their combinatorial fitness benefits are generally abated or their disadvantages amplified.

An analysis of epistasis in μ_{norm} (Supplementary Figure S11) and τ^{-1}_{norm} (Supplementary Figure S12) of each strain revealed that the magnitude of epistasis depended more heavily on the stress exposure, rather than the strain itself. Clustering analysis revealed that epistatic trends appeared to group by stress (Supplementary Figure S13). This was apparent especially under tetracycline exposure, which resulted in much larger degrees of negative epistasis in both μ_{norm} and τ^{-1}_{norm}. These findings could indicate disruption of stress-dependent adaptive pathways and poses an avenue for future research.

Interestingly, negative correlations between expected growth characteristics and their measured epistasis were also observed (Figure 6B). Removing the most negative value of epistasis still resulted in significant negative correlations ($r = -0.70$, $P = 2.4 \times 10^{-5}$ and $r = -0.79$, $P = 1.1 \times 10^{-7}$ for μ_{norm} and τ^{-1}_{norm} respectively). This implies that negative epistatic effects are strongest whenever multiple gene perturbations, which individually prove beneficial, are subsequently combined. This trend resembles diminishing returns epistasis, wherein the fitness gains of consecutive mutations decelerate during adaptation.[14,15] This phenomenon has been reproduced across a number of studies, and has been correlated to mutations which specifically impact gene expression.[45] It has been suggested that epigenetic epistatic interactions can constrain the evolution of gene expression.[17] The data presented here suggests an inherent fitness cost is associated with excessive perturbations of gene expression levels, and that epigenetic interactions may be subjected to the same diminishing returns epistasis typically associated with mutations.

DISCUSSION

Here we apply CRISPR technology, which thus far has been used primarily in a genome-editing capacity, to explore the effects of gene perturbations on bacterial adaptation. We demonstrate that minor (relative to previous studies[27,28]) perturbations in gene expression patterns are sufficient to reversibly alter bacterial fitness and growth characteristics during the early stages of stress exposure. We also identify significant negative epistasis when multiple genes are perturbed simultaneously. These results highlight the importance of gene expression in regulating bacterial adaptive responses and influencing the evolutionary pathways available during the early stages of stress exposure. This study also demonstrates a novel approach to rationally engineer control over bacterial fitness (and thus adaptive potential) without directly modifying the organism of interest.

Observed changes in gene expression during stress exposure have been extensively reported in bacteria.[46,47] We have recently demonstrated that *E. coli* grown under the same stress exhibits significant interpopulation heterogeneity in gene expression, where some genes demonstrate high expression variability while others are constrained within specific signatures.[11] This complexity surrounding differential gene expression during evolution demonstrates that bacteria have many avenues to explore their adaptive landscapes and develop novel, mutation-independent strategies to survive under stress.[48] Corroborating this notion is our finding that the phenotypic changes induced by gene perturbation during stress exposure are reversible upon the removal of stress, suggesting the importance of gene expression for the adaptive processes. It is important to note that all experimental strains of *E. coli* started from the same isogenic background (although harbored different CRISPR constructs) before exposure to stress. After exposure to stress, gene perturbations could likely influence the acquisition of mutations (as suggested by the increased mutation rates of MG1655-*soxS*a over MG1655-Control even in the absence of stress), resulting in heterogeneous end-population genotypes.

DOI: 10.1021/acssynbio.6b00050
ACS Synth. Biol. XXXX, XXX, XXX−XXX

Related efforts to study antimicrobial resistance has focused primarily on the effects of direct genetic modifications such as gene deletions or increased copy numbers via exogenous expression on a plasmid. For instance, the landmark genome-wide screen of Keio knockouts under 324 stress conditions by Nichols *et al.* enabled characterization of orphan genes' functions and connections within previously identified biological pathways.[27] Conversely, Soo *et al.* demonstrated that increasing gene copy numbers 300−400 fold utilizing the ASKA library increased the MIC in 115 cases.[28] While studies such as these and others[49] have been invaluable in relating gene function to survival under particular stresses, they employ genetic extremes (*i.e.*, complete gene knockouts or 300-fold gene copy increase) relative to the smaller changes in gene expression induced in this study. As such, their results less accurately represent what might be found in a distribution of a population of bacteria in nature. Our approach maintains the integrity of the original genome, while only introducing epigenetic changes via inducible transcriptional regulators. The degree of gene expression perturbation is also tunable; by changing the targeting site of the sgRNA, or the amount of aTc added to the system, one can adjust the efficiency of gene repression and activation.[20] Furthermore, a number of our results are consistent with previous studies. For instance, we observed that MG1655-*soxS*i exhibited decreased lag time under all five stress conditions, which is consistent with previous observations of *soxS* overexpression during lag phase[50] and could indicate that the superoxide stress response contributes to tolerance-by-lag.[39]

Interestingly, we also observed occasional phenotypic disconnect between activation and inhibition of gene targets, in that they did not impart contrasting phenotypes on adapting populations. For instance, MG1655-*dinB*i/a strains exhibited both beneficial and detrimental growth and fitness impacts, suggesting that DinB's error-prone activity is only conditionally beneficial. This is corroborated by confounding conclusions from previous studies, such as findings that *dinB*$^-$ exhibits increased fitness under certain antibiotics[27] but decreased fitness under others.[27] Indeed, we and others observe that perturbations (both genetic and epigenetic) impact fitness differently across a set of stresses. For instance, *acrA* and *tolC* have been shown to be up-regulated during the global stress response[51] but do not necessarily contribute to tolerance or can even promote increased fitness when knocked out.[27] We observe similar results in MG1655-*acrA*i/a, where inhibition reduced fitness in rifampicin but activation also reduced growth in nutrient starvation. A possible explanation for the disconnect between gene activation and inhibition across stresses could be that native gene expression is inherently large or small enough that skewing it further upward or downward respectively does not provide an adaptive advantage. This phenomenon has been postulated to explain the fact that the RpoS σ-factor does not induce *dinB* expression in response to ampicillin, as basal levels of DinB appear to be sufficient for ampicillin-induced mutagenesis.[52] However, this would not explain why both activation and inhibition of particular genes produced drastically different phenotypes over MG1655-Control. For instance, while previous studies have found *marA*$^-$ to decrease colony size[27] and *marA* hyper-expression to outcompete the wild-type[28] during tetracycline exposure, we find that in similar conditions both ∼10-fold *marA* inhibition and activation significantly increased τ. Thus, an alternate explanation is that gene targeting by these constructs disrupts regulatory pathways responsible for altering expression in response to environmental stress, such as the feedback network which has been postulated to control pulsation of *marA* expression.[53] This regulatory complexity, compounded by the connection of many of these genes within regulatory networks, obfuscates potential modular approaches to developing next-generation antimicrobial targets and highlights the need for studies such as this to better understand the consequences of artificial gene perturbation.

The canonical approach to study individual gene knockouts or duplications also neglects the combinatorial effects of multiple interacting genes. These effects are crucial in determining how adaptive trajectories unfold−the fixation of a mutation during the early stages of adaptation can constrain bacteria to a particular adaptive pathway that precludes another competing avenue of adaptation.[54] Previous studies have demonstrated that there is a pervasive tendency for coinciding bacterial mutations to display negative epistatic interactions.[14,15] Wright's shifting balance model predicts that epistasis plays a fundamental role in determining the likelihood of evolutionary drift overcoming fitness barriers to adaptation.[31,55] Utilizing our CRISPR-Cas9 based gene perturbation approach, we expand on this idea of negative epistasis controlling evolutionary pathways by discovering a striking correlation between concurrent perturbation of multiple genes' expression levels and negative epigenetic epistatic interactions. It should be noted that qPCR results demonstrate that there may have been a diminished gene expression impact from simultaneous gene perturbation than from individual gene perturbation, which could be a result of dCas9 (or dCas9-ω) protein being guided by multiple sgRNAs and thus diluting its concentration at individual genomic loci. However, this would not explain why the impacts of simultaneous gene perturbation were predominantly detrimental in nature, and might even suggest that greater negative epistatic trends might be encountered if dCas9 (or dCas9-ω) expression were to be increased to counteract potential sgRNA dilution effects. Regardless, this is the first reported observation of synthetically induced negative epistasis to the best of our knowledge. Just as negative epistatic interactions derived from mutations play a critical role in shaping bacterial adaptive trajectories, negative epigenetic epistatic interactions based on variations in gene expression also appear to be fundamentally important in shaping the availability of adaptive pathways[17] and should be taken into consideration when investigating how novel resistances evolve.

METHODS

Bacterial Strains, Media and Culture Conditions. *E. coli* cloning strains NEB 10-β (New England Biolabs) and DH5α (Zymo Research Corporation), as well as the final experimental strain K-12 MG1655 (ATCC 700926) were cultured in Luria−Bertani Broth (LB) (Sigma-Aldrich) unless otherwise noted. Colonies were grown on LB-agar plates supplemented with ampicillin (100 μg/mL) and chloramphenicol (25 μg/mL). For nutrient limiting conditions and growth of RT-qPCR biological triplicates, M9 minimal media (5X M9 minimal media salts solution from MP Biomedicals, 2.0 mM $MgSO_4$, and 0.1 mM $CaCl_2$ in sterile water) was used in lieu of LB, supplemented with 0.4% weight/vol glucose (34.2 mM). Expression of dCas9 and dCas9-ω was induced from plasmids pdCas9 and pPO-dCas9ω respectively by adding aTc (10 ng/mL) to the media. During competition experiments, aTc concentration was increased to 25 ng/mL to assist in distinguishing fluorescent

DOI: 10.1021/acssynbio.6b00050
ACS Synth. Biol. XXXX, XXX, XXX−XXX

populations from nonfluorescent ones. Cloning strains were made chemically competent with the *Mix & Go E. coli* Transformation Kit & Buffer Set (Zymo Research Corporation), and the final sgRNA plasmids were transformed into electrocompetent MG1655 cells harboring either pdCas9 or pPO-dCas9ω for inhibition or activation of gene expression, respectively. The final experimental strains are listed in Supplementary Table S3. Cultures (2−5 mL) were grown at 37 °C with constant shaking at 225 r.p.m. All experiments used biological triplicates inoculated from individual colonies grown on LB-agar plates supplemented with ampicillin and chloramphenicol.

Plasmid Assembly. A list of plasmids used in this study is provided in Supplementary Table S2. dCas9-ω from pWJ66 (Addgene plasmid 46570)[19] was first cloned into the same vector as dCas9 from pdCas9 (Addgene plasmid 44249)[20] under the same aTc inducible promoter, rrnB T1 terminator and chloramphenicol resistance marker to create plasmid pPO-dCas9ω. Single target sgRNA plasmids were first derived from the RFP-targeting control sgRNA-RFPi (Addgene plasmid 44251)[19] using the approach outlined in Supplementary Figure S9A. Primers were designed to replace the 44251 plasmid's RFP-targeting sgRNA using a common reverse primer (Reverse *sgRNA*) flanked with an *ApaI* restriction site and unique forward primers flanked with a *SpeI* restriction site, listed in Supplementary Table S4. PCR with Phusion High-Fidelity DNA Polymerase (New England Biolabs) was used to amplify these new target sgRNA-insert DNA fragments, which were subsequently gel-purified (Zymoclean Gel DNA Recovery Kit, Zymo Research Corporation), digested with *ApaI* and *SpeI* (FastDigest Enzymes, Thermo Scientific) as per the provided protocols and PCR-purified (GeneJET PCR Purification Kit, Thermo Scientific). The 44251 plasmid (Addgene) backbone was also digested with *ApaI* and *SpeI* and gel purified, and T4 DNA Ligase (Thermo Scientific) was used to ligate the new sgRNA target inserts into the 44251 backbone. Ligations were transformed into chemically competent DH5α or NEB 10-β cells. Plasmids minipreps were performed using Zyppy Plasmid Miniprep Kit (Zymo Research Corporation). Sequencing of final sgRNA constructs were performed for validation of correct assembly product (GENEWIZ).

To create the fluorescent control for competition assays, mCherry from pHL662 (Addgene plasmid 37636) was PCR amplified with *AatII* restriction sites on either end of the resulting fragment, and cloned onto sgRNA-RFPi under an aTc inducible promoter. This construct was transformed into MG1655 harboring pdCas9 to create MG1655-mCherry.

To create multigene targeting sgRNA plasmids, the above single gene targeting sgRNAs were combined using the procedure outlined in Supplementary Figure S9B. The first sgRNA target plasmid was digested with *Bam*HI and *XbaI* and the 2569 bp vector was gel-purified. A second target plasmid was digested using *Bgl*II and *XbaI* and the 527 bp insert was gel-purified. These were ligated and transformed into DH5α chemically competent cells and plated on LB-ampicillin plates. *Bam*HI and *Bgl*II digestion overhangs produce compatible sticky ends that, when ligated together, do not produce a new restriction enzyme site. After recovering these plasmids, a *Bam*HI digestion was used to confirm the plasmids were the correct size on an agarose gel. To create more than two targets, the same approach was applied using the *Bam*HI/*XbaI* digestion on the two gene targeting plasmid and the *Bgl*II/*XbaI* digestion on the third target. All inserted fragments were confirmed by sequencing.

RT-qPCR Analysis. Biological triplicate cultures inoculated from individual colonies were grown with appropriate antibiotics overnight in 2.5 mL M9 minimal media. Cultures were induced with aTc the following morning for 3 h, and cell pellets were subsequently collected and RNA extracted using the GeneJET RNA Purification Kit (Thermo Scientific) supplemented with lysozyme and proteinase K. Collected RNA was then purified using the TURBO DNA-free kit (Ambion) for heavy DNA contamination. cDNA was synthesized from these RNA samples using 10 μL reactions of the DyNAmo SYBR Green 2-Step qRT-PCR kit (Thermo Scientific). A control reverse-transcriptase-free reaction was included in tandem with all cDNA synthesis reactions. Technical duplicates of RT-qPCR reactions were performed in 10 μL reactions using 2 ng of cDNA and 0.5 μM primers listed in Supplementary Table S5. Primer efficiency and specificity were confirmed in a previous experiment.[11] Samples were run on an Eco Real-Time PCR System (Illumina) in the CU Core Sequencing Facility operating the Eco Software v4.1.2.0. RT-qPCR reactions of neighboring genes' expression were performed in 20 μL using 2 ng of cDNA and 0.5 μM primers, and were run on a QuantStudio 6 Flex Real-Time PCR System (Thermo Scientific) in the CU Core Sequencing Facility. An initial 10 min polymerase activation at 95 °C was performed, followed by 40 cycles of 95 °C 15 s denaturation, 55 °C 30 s annealing, and 72 °C 30 s extension. Rox normalization was used to compare qPCR samples, and the average C_q values of technical duplicates were used to calculate the $\Delta\Delta C_q$ values using *rrsA* gene expression as a housekeeping gene, which was also averaged. Fold change was calculated using $2^{-\Delta\Delta Cq}$ values for individual biological triplicates, which were subsequently used to obtain averages and standard deviations.

MIC Determination. MICs were first determined via overnight growths of MG1655 harboring dCas9 and RFP-targeting sgRNA with no induction, and measuring the change in OD at 562 nm. A range of concentrations for the disinfectants (hydrogen peroxide and bleach) and the antibiotics (rifampicin and tetracycline) were tested (Supplementary Figure S4). MIC tests started at concentrations of 74.6 mM, 20.4 mM, 10 ng/μL and 100 ng/μL for bleach, hydrogen peroxide, rifampicin and tetracycline, respectively. MICs were determined to be the lowest concentration which prevented a change of 0.1 OD between days. The final sub-MIC values used in this experiment, as well as a description of mechanisms of action, are presented Figure 2A.

Stress conditions were selected to monitor a broad range of antimicrobials. Peroxide and bleach introduce oxidative stress by producing highly reactive superoxide[35] or chlorine[34] radicals, respectively. Tetracycline inhibits protein synthesis by disrupting tRNA interactions with the ribosome,[36] while rifampicin inhibits transcription by preventing the activity of RNA polymerase.[37] These antibiotics avoided mechanistic overlap with the antibiotics required to maintain plasmid selection, ampicillin and chloramphenicol, which inhibit cell-wall-synthesis and peptide bond formation, respectively.

Stress Growth Conditions. Biological triplicates were inoculated from individual colonies of MG1655 cultures harboring both dCas9/dCas9-ω and sgRNA plasmids into 100 μL LB cultures supplemented with ampicillin, chloramphenicol and aTc and grown overnight to stationary phase. The next day, 2 μL was used to inoculate one 50 μL M9 culture and

DOI: 10.1021/acssynbio.6b00050
ACS Synth. Biol. XXXX, XXX, XXX−XXX

five 50 μL LB cultures in a 384-well microplate, all of which were supplemented with aTc and the appropriate antibiotics. Four of the LB cultures were supplemented with either 37.3 mM sodium hypochlorite (BLEACH-RITE, Current Technologies), 0.3 mM hydrogen peroxide (Macron Fine Chemicals), 1.0 ng/μL tetracycline (Sigma-Aldrich), or 10.0 ng/μL rifampicin (Sigma-Aldrich) respectively. Bleach stress was increased to 74.6 mM and 149.2 mM on days two and three respectively, and peroxide stress was increased to 0.6 mM on days two and three to maintain selection pressure. Cultures for subsequent experimental days were created as described above and inoculated with 2 μL of the previous day's culture. Culture growth was monitored in 384 microplate wells in a GENios plate reader (Tecan Group Ltd.) operating under the Magellan software (version 7.2).

Optical densities were measured at 562 nm absorbance in 20 min intervals. Temperature was maintained at 37 °C, and cultures were shaken for 16.6 min after each measurement with an additional 10 s of shaking before measurement. Data output was used to construct raw growth curves over multiple days (Supplementary Figure S3), and growth rates (μ) and lag times (τ) were determined using the *GrowthRates* version 1.8[56] and calculated for each day (SI Extended Data Set). This program estimates the period of exponential growth and excludes lag and stationary phases from calculation of μ. Data were normalized to the performance of strain MG1655-Control over the course of 3 days. After normalization, lag times were inverted to simplify analysis for the reader. As larger lag times are considered detrimental, inverting these values made values below 1.0 appear detrimental, as they are for growth rates. Distance from $\mu_{norm} = 1.0$, $\tau^{-1}{}_{norm} = 1.0$ on each graph was calculated as $D = \sum_n \sqrt{(\mu_n - 1)^2 + (\tau^{-1}{}_{n^{-1}})^2}$, where n is each of the seven inhibition or activation perturbations strains from their respective graphs.

At the end of adaptation experiments, glycerol stocks of cultures were saved. For re-adaptation experiments, glycerol stocks of the original biological triplicates were streaked onto LB agar plates containing antibiotics and grown overnight. Individual colonies were used to inoculate LB cultures containing antibiotics and grown for 16 h. Afterward, cultures were diluted 1:10 into fresh LB containing antibiotics and grown for 24 h. From this point, the protocol for the original three-day adaptation experiment was performed for cultures under no stress, no stress and aTc induction, and the original stress condition (rifampicin or tetracycline) and aTc induction.

Competitive Fitness Assays. Gene perturbation strains MG1655-*mutS*a, MG1655-*dinB*i, MG1655-*acrA*i and MG1655-*mutS*a-*dinB*i, as well as the control strain MG1655-Control, were competed against MG1655-mCherry. mCherry fluorescence measured at 610 nm was used to distinguish the two populations during competition experiments using FACS. To measure the fitness of experimental strains relative to MG1655-mCherry, 2 mL LB (or M9 + 0.4% glucose) cultures supplemented with ampicillin, chloramphenicol and aTc were inoculated from individual colonies and grown overnight for 16 h. The cultures were then diluted 1:10 in supplemented LB (or M9 + 0.4% glucose) and grown for 2 h. Culture ODs (at 562 nm) were then measured and used to mix the two cultures together at either 1:1 or 3:7 OD ratio as indicated in the figures and text. A total of 200 μL of cultures were mixed, out of which 10 μL was added to 190 μL of each stress or no stress condition per biological replicate. The remaining volume was used for FACS analysis of pre-experiment starting population distributions (D0). Cultures were grown in 96-well microplates in the GENios plate reader as described previously for 1 day, and the final cultures were collected for FACS analysis.

Relative fitness was determined using the ratio of Malthusian parameters (m) of each experimental strain against m of competitor strain MG1655-mCherry, as previously described.[41] Malthusians were calculated as $m = \ln(N_f/N_i)$ where N_f and N_i are the number of final and initial cells in each mixture, respectively. Initial and final cell counts were determined from FACS analysis, and adjusted to represent their respective dilutions.

Flow Cytometry. Samples for FACS analysis were washed twice in phosphate-buffered saline (PBS) and resuspended in PBS + 4.0% (vol/vol) para-formaldehyde (Fisher Scientific). Samples were diluted 1:10 in PBS and sorted using a CyAn ADP analyzer cytometer. Samples were kept on ice throughout the procedure. From each sample 100,000 cells were counted using a voltage of 920 V in a PE-Texas Red channel, a forward scatter gain of 40, and a side scatter voltage of 550 V for detection of mCherry fluorescence. Cells which fluoresced above an intensity of 20 were determined to be MG1655-mCherry, while those below 20 were determined to be the experimental strains. FACS data was analyzed using Matlab and Summit software.

Sequencing of Experimental Strains. For sequencing of genes directly targeted by CRISPR constructs, glycerol stocks of cultures saved at the end of 3 days of stress exposure were streaked onto LB agar plates containing antibiotics. Two colonies from each biological replicate were picked and used to perform colony PCR using Phusion high-fidelity DNA polymerase. Primers used for these reactions are listed in Supplementary Table S4, and resulted in the fragments listed. PCR products were subsequently gel-purified. Sequencing reactions were performed using each reverse primer by GENEWIZ. Sequences were aligned to *E. coli* MG1655 NCBI reference genome NC_000913 using NCBI BLASTN.

Mutation Fluctuation Assay. Overall mutation rates of a subset of strains were determined using a mutation fluctuation assay as outlined by Luria and Delbrück.[57] Briefly, single colonies of each strain were picked from LB agar plates supplemented with chloramphenicol and ampicillin and grown overnight for 16 h in 1 mL LB without selection. These cultures were then adjusted to the same optical densities via addition of LB to denser cultures, and diluted 1:10,000 into 30 three parallel 100 μL cultures of LB supplemented with ampicillin, chloramphenicol and aTc. After 24 h of growth, three cultures were plated in dilutions on LB agar to determine colony forming units. The remaining 30 cultures were plated on LB agar plates supplemented with 100 μg/mL of rifampicin. Colonies on each plate were counted after 24 h of growth in 37 °C and used to determine mutation rates. Rates were calculated using the FALCOR web tool.[58]

Determination of Epistasis. Expected growth rates were calculated assuming a multiplicative model[59] of deviations from the relative control values: for example, $\mu_{Expected,\ gene12} = \mu_{gene1} \times \mu_{gene2}$, where μ_{gene1} represents the growth rate observed in the strain targeting gene 1 individually. This provided the expected shift in growth rates (with respect to MG1655-Control) of the multigene targeting strains based on results from their individual gene targeting strains. Epistasis when combining perturbation of gene "*a*" and "*b*" was calculated as the difference between the observed relative growth rate of the multitarget

DOI: 10.1021/acssynbio.6b00050
ACS Synth. Biol. XXXX, XXX, XXX−XXX

strains and the calculated expected growth Epistasis$_{ab}$ = $\mu_{observed,ab} - \mu_{expected,ab}$ where $\mu_{expected,ab} = \mu_a{}^*\mu_b$). Calculations of epistasis in inverse lag times were analogous to this procedure. Epistasis was calculated for all five strains with simultaneously perturbed gene expression under all six growth conditions based on the average values presented in SI Extended Data Set. The 95% confidence interval for average fitness epistasis was calculated using standard error. A z-test was performed to calculate the probability that this deviated from the null hypothesis of no epistasis, and the resulting *P*-value was obtained assuming a two-tailed distribution.

■ ASSOCIATED CONTENT

Supporting Information

The Supporting Information is available free of charge on the ACS Publications website at DOI: 10.1021/acssynbio.6b00050.

Figures S1−S13; Tables S1−S5; lists of all the cloning, sequencing, and qPCR primers used in this study, all plasmids and strains used in this study, and extended description of all of the genes investigated, the binding sequences of each sgRNA target site, additional qPCR data of neighboring genes, control growth curves, experimental setup, analysis of growth rate and lag time dependency, supporting FACS data, and further analysis of epistatic trends (PDF)

Extended Data Set; Tabulated growth rate and lag time information for each strain (XLSX)

■ AUTHOR INFORMATION

Corresponding Author

*E-mail: chatterjee@colorado.edu. Phone: (303) 735-6586. Fax: (303) 492-8425.

Author Contributions

P.B.O. performed all experiments. K.E.E. and P.B.O. designed sgRNA constructs, and P.B.O generated dCas9-ω and sgRNA constructs and strains. A.E.B. collected and analyzed FACS data. K.E.E. designed RT-qPCR sequencing primers. A.C. and P.B.O. conceived of experiments, and P.B.O. and K.E.E. designed experiments. P.B.O. and A.C. wrote the manuscript.

Notes

The authors declare no competing financial interest.

■ ACKNOWLEDGMENTS

We would like to thank Jamie Prior Kershner for use of the Eco Illumina machine in the CU Core Sequencing Facility. The authors acknowledge financial support for this work from the National Science Foundation Graduate Research Fellowship (Award #DGE1144083) to PBO, the National Institute of Health Pharmaceutical Biotechnology Fellowship (Grant #5T32GM008732) to KEE, Balsells Graduate Fellowship to AEB, the William M. Keck Foundation (Grant #OCG6145B) to AC, and University of Colorado start-up funds to A.C.

■ REFERENCES

(1) Chatterjee, A., et al. (2013) Antagonistic self-sensing and mate-sensing signaling controls antibiotic-resistance transfer. *Proc. Natl. Acad. Sci. U. S. A. 110*, 7086−7090.

(2) Pericone, C. D., Park, S., Imlay, J. A., and Weiser, J. N. (2003) Factors contributing to hydrogen peroxide resistance in Streptococcus pneumoniae include pyruvate oxidase (SpxB) and avoidance of the toxic effects of the Fenton Reaction. *J. Bacteriol. 185*, 6815−6825.

(3) CDC (2013) *Antibiotic resistance threats in the United States, 2013*, U.S. Department of Health and Human Services.

(4) Raser, J. M., and O'Shea, E. K. (2005) Noise in gene expression: origins, consequences, and control. *Science 309*, 2010−2013.

(5) Raj, A., and van Oudenaarden, A. (2008) Nature, Nurture, or Chance: stochastic gene expression and its consequences. *Cell 135*, 216−226.

(6) López-Maury, L., Marguerat, S., and Bähler, J. (2008) Tuning gene expression to changing environments: from rapid responses to evolutionary adaptation. *Nat. Rev. Genet. 9*, 583−593.

(7) Beaumont, H. J. E., Gallie, J., Kost, C., Ferguson, G. C., and Rainey, P. B. (2009) Experimental evolution of bet hedging. *Nature 462*, 90−93.

(8) Fernández, L., Breidenstein, E. B. M., and Hancock, R. E. W. (2011) Creeping baselines and adaptive resistance to antibiotics. *Drug Resist. Updates 14*, 1−21.

(9) Kaldalu, N., Mei, R., and Lewis, K. (2004) Killing by ampicillin and ofloxacin induces overlapping changes in Escherichia coli transcription profile. *Antimicrob. Agents Chemother. 48*, 890−896.

(10) Ceragioli, M., et al. (2010) Comparative transcriptomic and phenotypic analysis of the responses of Bacillus cereus to various disinfectant treatments. *Appl. Environ. Microbiol. 76*, 3352−3360.

(11) Erickson, K. E., Otoupal, P. B., and Chatterjee, A. (2015) Gene Expression Variability Underlies Adaptive Resistance in Phenotypically Heterogeneous Bacterial Populations. *ACS Infect. Dis. 1*, 555−567.

(12) Fong, S. S., Joyce, A. R., and Palsson, B. Ø. (2005) Parallel adaptive evolution cultures of Escherichia coli lead to convergent growth phenotypes with different gene expression states. *Genome Res. 15*, 1365−1372.

(13) Puentes-Téllez, P. E., Kovács, Á. T., Kuipers, O. P., and van Elsas, J. D. (2014) Comparative genomics and transcriptomics analysis of experimentally evolved Escherichia coliMC1000 in complex environments. *Environ. Microbiol. 16*, 856−870.

(14) Khan, A. I., Dinh, D. M., Schneider, D., Lenski, R. E., and Cooper, T. F. (2011) Negative epistasis between beneficial mutations in an evolving bacterial population. *Science 332*, 1193−1196.

(15) Chou, H.-H., Chiu, H.-C., Delaney, N. F., Segrè, D., and Marx, C. J. (2011) Diminishing returns epistasis among beneficial mutations decelerates adaptation. *Science 332*, 1190−1192.

(16) Woods, R. J., et al. (2011) Second-order selection for evolvability in a large Escherichia coli population. *Science 331*, 1433−1436.

(17) Park, S., and Lehner, B. (2013) Epigenetic epistatic interactions constrain the evolution of gene expression. *Mol. Syst. Biol. 9*, e645.

(18) Sander, J. D., and Joung, J. K. (2014) CRISPR-Cas systems for editing, regulating and targeting genomes. *Nat. Biotechnol. 32*, 347−55.

(19) Qi, L. S., et al. (2013) Repurposing CRISPR as an RNA-guided platform for sequence-specific control of gene expression. *Cell 152*, 1173−1183.

(20) Bikard, D., et al. (2013) Programmable repression and activation of bacterial gene expression using an engineered CRISPR-Cas system. *Nucleic Acids Res. 41*, 7429−7437.

(21) Randall, L. P., and Woodward, M. J. (2002) The multiple antibiotic resistance (mar) locus and its significance. *Res. Vet. Sci. 72*, 87−93.

(22) Duval, V., and Lister, I. M. (2013) MarA, SoxS and Rob of Escherichia coli − Global regulators of multidrug resistance, virulence and stress response. *Int. J. Biotechnol. Wellness Ind. 2*, 101−124.

(23) Giese, K. C., Michalowski, C. B., and Little, J. W. (2008) RecA-dependent cleavage of LexA dimers. *J. Mol. Biol. 377*, 148−161.

(24) Giraud, A., et al. (2001) Costs and benefits of high mutation rates: adaptive evolution of bacteria in the mouse gut. *Science 291*, 2606−2608.

(25) Galhardo, R. S., et al. (2009) DinB upregulation is the sole role of the SOS response in stress-induced mutagenesis in Escherichia coli. *Genetics 182*, 55−68.

(26) Pérez, A., et al. (2007) Cloning, nucleotide sequencing, and analysis of the AcrAB-TolC efflux pump of Enterobacter cloacae and

DOI: 10.1021/acssynbio.6b00050
ACS Synth. Biol. XXXX, XXX, XXX−XXX

determination of its involvement in antibiotic resistance in a clinical isolate. *Antimicrob. Agents Chemother. 51*, 3247−3253.
(27) Nichols, R. J., et al. (2011) Phenotypic landscape of a bacterial cell. *Cell 144*, 143−156.
(28) Soo, V. W. C., Hanson-Manful, P., and Patrick, W. M. (2011) Artificial gene amplification reveals an abundance of promiscuous resistance determinants in Escherichia coli. *Proc. Natl. Acad. Sci. U. S. A. 108*, 1484−1489.
(29) Isalan, M., et al. (2008) Evolvability and hierarchy in rewired bacterial gene networks. *Nature 452*, 840−845.
(30) Barrick, J. E., et al. (2009) Genome evolution and adaptation in a long-term experiment with Escherichia coli. *Nature 461*, 1243−7.
(31) Phillips, P. C. (2008) Epistasis - the essential role of gene interactions in the structure and evolution of genetic systems. *Nat. Rev. Genet. 9*, 855−867.
(32) González, C., et al. (2015) Stress-response balance drives the evolution of a network module and its host genome. *Mol. Syst. Biol. 11*, 827.
(33) Nevozhay, D., Adams, R. M., van Itallie, E., Bennett, M. R., and Balázsi, G. (2012) Mapping the environmental fitness landscape of a synthetic gene circuit. *PLoS Comput. Biol. 8*, e1002480.
(34) Gray, M. J., Wholey, W.-Y., and Jakob, U. (2013) Bacterial responses to reactive chlorine species. *Annu. Rev. Microbiol. 67*, 141−160.
(35) Linley, E., Denyer, S. P., McDonnell, G., Simons, C., and Maillard, J.-Y. (2012) Use of hydrogen peroxide as a biocide: new consideration of its mechanisms of biocidal action. *J. Antimicrob. Chemother. 67*, 1589−1596.
(36) Chopra, I., and Roberts, M. (2001) Tetracycline antibiotics: mode of action, applications, molecular biology, and epidemiology of bacterial resistance. *Microbiol. Mol. Biol. Rev. 65*, 232−260.
(37) Campbell, E. A., et al. (2001) Structural mechanism for rifampicin inhibition of bacterial RNA polymerase. *Cell 104*, 901−912.
(38) Andersson, D. I. (2003) Persistence of antibiotic resistant bacteria. *Curr. Opin. Microbiol. 6*, 452−456.
(39) Fridman, O., Goldberg, A., Ronin, I., Shoresh, N., and Balaban, N. Q. (2014) Optimization of lag time underlies antibiotic tolerance in evolved bacterial populations. *Nature 513*, 418−421.
(40) Gall, S., Lynch, M. D., Sandoval, N. R., and Gill, R. T. (2008) Parallel mapping of genotypes to phenotypes contributing to overall biological fitness. *Metab. Eng. 10*, 382−393.
(41) Lenski, R. E., Rose, M. R., Simpson, S. C., and Tadler, S. C. (1991) Long-Term Experimental Evolution in Escherichia Coli. Adaptation and Divergence During 2,000 Generations. *Am. Nat. 138*, 1315−1341.
(42) Gama-Castro, S., et al. (2016) RegulonDB version 9.0: high-level integration of gene regulation, coexpression, motif clustering and beyond. *Nucleic Acids Res. 44*, gkv1156.
(43) Zalatan, J. G., et al. (2014) Engineering complex synthetic transcriptional programs with CRISPR RNA scaffolds. *Cell 160*, 339−350.
(44) Farzadfard, F., Perli, S. D., and Lu, T. K. (2013) Tunable and multifunctional eukaryotic transcription factors based on CRISPR/Cas. *ACS Synth. Biol. 2*, 604−613.
(45) Chou, H. H., Delaney, N. F., Draghi, J. a., and Marx, C. J. (2014) Mapping the fitness landscape of gene expression uncovers the cause of antagonism and sign epistasis between adaptive mutations. *PLoS Genet. 10*, e1004149.
(46) Pomposiello, P. J., Bennik, M. H. J., and Demple, B. (2001) Genome-wide transcriptional profiling of the Escherichia coli responses to superoxide stress and sodium salicylate. *J. Bacteriol. 183*, 3890.
(47) Cooper, T. F., Rozen, D. E., and Lenski, R. E. (2003) Parallel changes in gene expression after 20,000 generations of evolution in Escherichia coli. *Proc. Natl. Acad. Sci. U. S. A. 100*, 1072−1077.
(48) Sánchez-Romero, M. A., and Casadesús, J. (2014) Contribution of phenotypic heterogeneity to adaptive antibiotic resistance. *Proc. Natl. Acad. Sci. U. S. A. 111*, 355−60.
(49) Kondrashov, F. a. (2012) Gene duplication as a mechanism of genomic adaptation to a changing environment. *Proc. R. Soc. London, Ser. B 279*, 5048−5057.
(50) Rolfe, M. D., et al. (2012) Lag phase is a distinct growth phase that prepares bacteria for exponential growth and involves transient metal accumulation. *J. Bacteriol. 194*, 686−701.
(51) Rosenberg, E. Y., et al. (2003) *Mol. Microbiol. 48*, 1609−1619.
(52) Gutierrez, a, et al. (2013) *β*-Lactam antibiotics promote bacterial mutagenesis via an RpoS-mediated reduction in replication fidelity. *Nat. Commun. 4*, 1610.
(53) Garcia-Bernardo, J., and Dunlop, M. J. (2013) Tunable Stochastic Pulsing in the Escherichia coli Multiple Antibiotic Resistance Network from Interlinked Positive and Negative Feedback Loops. *PLoS Comput. Biol. 9*, e1003229.
(54) Tenaillon, O., et al. (2012) The molecular diversity of adaptive convergence. *Science 335*, 457−461.
(55) Wright, S. (1932) The roles of mutation, inbreeding, crossbreeding and selection in evolution. *Proc. Sixth Int. Congr. Genet.*, 356.
(56) Hall, B. G., Acar, H., Nandipati, A., and Barlow, M. (2014) Growth rates made easy. *Mol. Biol. Evol. 31*, 232−238.
(57) Luria, S. E., and Delbruck, M. (1943) Mutations of bacteria from virus sensitivity to virus resistance. *Genetics 28*, 491−511.
(58) Hall, B. M., Ma, C.-X., Liang, P., and Singh, K. K. (2009) Fluctuation AnaLysis CalculatOR: a web tool for the determination of mutation rate using Luria-Delbruck fluctuation analysis. *Bioinformatics 25*, 1564−1565.
(59) Trindade, S., et al. (2009) Positive epistasis drives the acquisition of multidrug resistance. *PLoS Genet. 5*, e1000578.

DOI: 10.1021/acssynbio.6b00050
ACS Synth. Biol. XXXX, XXX, XXX−XXX